2016

Developing the Surface Chemistry of Transparent Butyl Rubber for Impermeable Stretchable Electronics

Tricia Carmichael
University of Windsor

Akhil Vohra
University of Windsor

R. Stephen Carmichael
University of Windsor

Developing the Surface Chemistry of Transparent Butyl Rubber for Impermeable Stretchable Electronics

*Akhil Vohra, R. Stephen Carmichael and Tricia Breen Carmichael**

Department of Chemistry & Biochemistry, University of Windsor, Windsor, ON, Canada, N9B 3P4

tbcarmic@uwindsor.ca

Abstract

Transparent butyl rubber is a new elastomer that has the potential to revolutionize stretchable electronics due to its intrinsically low gas permeability. Encapsulating organic electronic materials and devices with transparent butyl rubber protects them from problematic degradation due to oxygen and moisture, preventing premature device failure and enabling the fabrication of stretchable organic electronic devices with practical lifetimes. Here, we report a methodology to alter the surface chemistry of transparent butyl rubber to advance this material from acting as a simple device encapsulant to functioning as a substrate primed for direct device fabrication on its surface. We demonstrate a combination of plasma and chemical treatment to deposit a hydrophilic silicate layer on the transparent butyl rubber surface to create a new layered composite that combines Si-OH surface chemistry with the favorable gas-barrier properties of bulk transparent butyl rubber. We demonstrate that these surface Si-OH groups react with organosilanes to form self-assembled monolayers necessary for the deposition of electronic materials, and furthermore demonstrate the fabrication of stretchable gold wires using nanotransfer printing of gold films onto transparent butyl rubber modified with a thiol-terminated self-assembled monolayer. The surface modification of transparent butyl rubber establishes this material as an important new elastomer for stretchable electronics and opens the way to robust, stretchable devices.

Introduction

Stretchable electronic devices are built to function during stretching, bending, and twisting.[1-2] This field of research has produced exciting new technologies that are conformable, wearable, or implantable into the body, such as stretchable light-emitting devices and displays,[3-7] organic photovoltaics (OPVs),[8] wearable strain sensors and health monitors,[9-11] and implantable biosensors.[12] The key to producing stretchable devices is the careful integration of functional electronic materials with elastomeric substrates,[13] usually by depositing thin films of the desired functional material onto the surface of the elastomer. These films retain electrical function during stretching by manipulating the pattern of crack formation in the film with stretching;[14-17] structuring the films on the elastomer surface into serpentine patterns, fractal-inspired layouts, topographic buckles, or pop-up structures;[18-22] or designing new functional materials that are intrinsically stretchable.[23] Regardless of the method used, the interface between the electronic material and elastomer is a critically important parameter. The electronic material must effectively wet the elastomer surface to form a film in the first place; moreover, the adhesion between the two materials defines how well the structure retains electrical functionality with strain. When the structure is stretched, strain localization in a poorly adhered film results in delamination from the elastomer surface to form free-standing regions that experience large local strains and fracture easily, leading to the formation of channel cracks that propagate along the film and destroy pathways for charge transport.[23-26] On the other hand, strong adhesion between the film and elastomer suppresses strain localization and delamination, allowing the film to deform uniformly and limiting crack propagation.[14,27-28] It is therefore crucial to be able to modify the chemistry and free energy of the elastomer surface to facilitate wetting and adhesion.

Poly(dimethylsiloxane) (PDMS) has been the elastomer of choice for stretchable electronics for several reasons, such as optical transparency (100% transmittance @550 nm), commercial availability, and simple molding procedures.[29] Most importantly, it is remarkably easy to modify and tailor the surface chemistry of PDMS to enable film wetting and adhesion (Scheme 1a). Simple air or oxygen plasma treatment of PDMS creates a thin, hydrophilic silicate layer (θ_{H2O} < 20°) on the surface that enables wetting and adhesion of materials.[30] Furthermore, the -OH terminal groups of the silicate surface readily react with ω-functionalized organosilanes through condensation reactions to form self-assembled monolayers (SAMs) that are anchored by Si-O-Si siloxane bonds and present specific functional groups to enable the deposition and adhesion of materials.[31-32] For example, thiol-terminated silane SAMs on PDMS act as an interfacial adhesion layer to bind metal films to the PDMS surface through the formation of covalent metal-sulfur bonds.[33-34] Amino-terminated silanes on PDMS bind colloidal catalysts to enable the electroless deposition of stretchable copper films on the surface,[35] or act as a base layer for the deposition of transparent and conductive carbon nanotube films.[36] Organosilane initiator molecules on PDMS can be used to initiate the growth of polymer brushes on the surface.[37-38]

Scheme 1. Surface modification of (a) PDMS and (b) T-IIR and subsequent formation of an organosilane SAM.

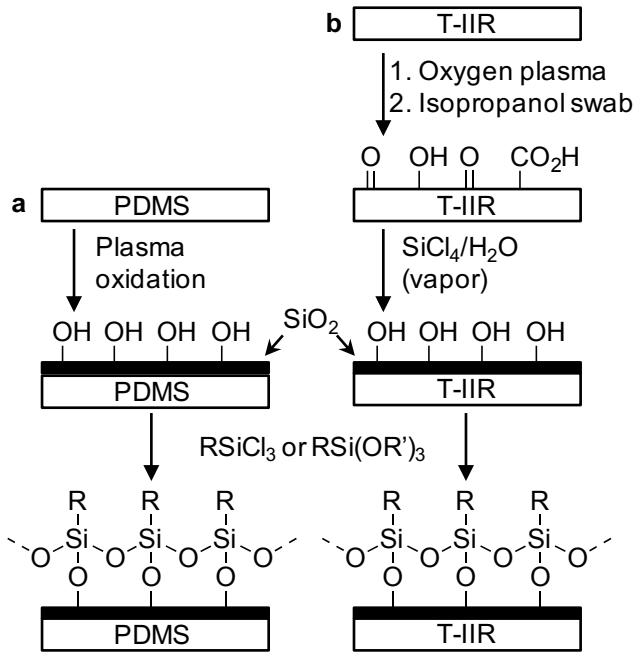

The ease with which the surface properties of PDMS can be modified is undeniably a strong motivator for the use of PDMS in stretchable electronics; however, it is a bulk property – gas permeability – that is the most significant detriment to PDMS in many stretchable electronics applications. We recently reported that the high permeability of PDMS to oxygen and water vapor readily permits the oxidation and/or hydrolysis of organic device materials such as semiconducting organic molecules and polymers, and the oxidation and corrosion of metals such as silver or copper,[39] which will curtail the lifetime of devices such as organic light-emitting devices and organic photovoltaics.[40-42] To solve this problem, we have reported a new elastomer for stretchable electronics that possesses an intrinsically low gas permeability to protect sensitive device components. This material is a new formulation of butyl rubber (poly(isobutylene-co-isoprene),

IIR) consisting of a peroxide-cured IIR ionomer that can be compression molded to produce optically transparent (80% transmittance @550 nm) and clear butyl rubber sheets.[39] Like the conventional butyl rubber typically used in automobile tires and pharmaceutical stoppers, the high gas impermeability of this new transparent butyl rubber (T-IIR) arises from methyl groups on the polymer backbone, which impede the movement of the polymer chains and reduce the ability of gas molecules to pass through the material.[43-44] The oxygen permeation rate of T-IIR (216 ± 3 cc-mm/m^2-day) is more than an order of magnitude lower than that of PDMS (4500 cc-mm/m^2-day). We have demonstrated that T-IIR is an effective gas-barrier layer that vastly outperforms PDMS when used as an encapsulant to protect sensitive electronic materials and devices from degradation due to gas permeation.[39]

For T-IIR to be used as a high-gas barrier elastomer in stretchable electronics, however, it must advance from being used simply as an encapsulant to functioning as a substrate for device fabrication. It is therefore critical to develop methods to modify the surface chemistry of T-IIR to enable wetting and adhesion of functional device materials. T-IIR surface modification, however, is not trivial. Simply implementing the surface modification protocol used for PDMS is complicated by the fact that T-IIR is a hydrocarbon elastomer that cannot form a hydrophilic silicate layer on its surface by simple plasma oxidation. Moreover, plasma and chemical (chromic acid or potassium permanganate) oxidation both damage T-IIR, producing oxidized products of chain scission that remain physisorbed on the surface.[45] Here, we report a new process to modify the T-IIR surface in which we use a combination of plasma treatment, solvent-assisted removal of physisorbed scission products, and chemical treatment to deposit a hydrophilic silicate layer on the T-IIR surface, creating a new layered composite (T-IIR$_{[ox]}$/SiO_2) that combines Si-OH surface chemistry similar to that of oxidized PDMS with the favorable gas-barrier properties of bulk T-

IIR (Scheme 1b). We demonstrate that the Si-OH groups on the surface of T-IIR$_{[ox]}$/SiO_2 composites react with organosilanes to form SAMs that enable the deposition of electronic materials.

Experimental Section

All chemicals were obtained from Sigma-Aldrich and were used as received. T-IIR substrates and PDMS stamps were prepared according to published procedures.[39,46]

Fabrication of T-IIR$_{[ox]}$/SiO_2 Substrates T-IIR substrates (~0.5 mm thick, 6.0 × 6.0 cm^2) were sonicated in acetone and isopropanol for 10 min each, and then treated with oxygen plasma for 15 min in a Harrick plasma cleaner at O_2 pressure of 10 psig and flow rate of 10.6 $mL \cdot min^{-1}$ at medium discharge setting. The oxidized samples were swabbed with isopropanol, dried in a stream of nitrogen, and suspended for 30 s over a glass Petri dish containing 0.1 mL of silicon tetrachloride in ambient conditions. The samples were then soaked in DI H_2O for 10 min, and dried in a stream of nitrogen.

Fabrication of Self-Assembled Monolayers (SAMs) SAMs of trichloro(1H,1H,2H,2H-perfluorooctyl)silane (FOTS), 3-mercaptopropyltrimethoxysilane (MPTMS), and n-octadecyltrichlorosilane (OTS) were deposited on T-IIR$_{[ox]}$/SiO_2 substrates suspended over a 250 mL beaker containing 3-5 drops of organosilane in a vacuum desiccator for 20 h. SAMs of 3-aminopropyltriethoxysilane (APTES) were deposited by immersing T-IIR$_{[ox]}$/SiO_2 substrates in 1% v/v APTES solution in DI H_2O.

Nanotransfer Printing (nTP) A 1000-Å-thick film of Au was deposited by e-beam evaporation at a rate of 2.0 Å/s onto a PDMS stamp or through a stainless steel mask with 1 mm x 10 mm opening onto a flat PDMS stamp. The PDMS stamps were then brought into conformal

contact with MPTMS-treated T-IIR$_{[ox]}$/SiO_2 for 1 min. Fast removal of the stamp from the T-IIR$_{[ox]}$/SiO_2/MPTMS substrate completes the transfer of the Au film onto T-IIR.

Characterization Water contact angles were measured using the sessile drop method on a Ramé-Hart contact angle goniometer. At least four drops from three samples were averaged. Attenuated Total Reflectance Fourier Transform Infrared Spectroscopy (ATR-FTIR) spectra were collected using a Bruker IFS 66/v spectrometer equipped with a DTGS detector. The p-polarized light was incident at 45° from the surface normal. For each sample, 2048 scans were collected at a resolution of 4 cm^{-1} using a ZnSe crystal. X-ray Photoelectron Spectroscopic (XPS) analysis was done using a Kratos Axis Nova X-ray photoelectron spectrometer at Surface Science Western, London, Ontario. XPS survey spectra were obtained from an area of approximately 300 μm x 700 μm using a pass energy of 160 eV. A 90-degree take-off angle was used. Transmittance spectra were measured using a Varian Cary 50 UV-Visible Spectrophotometer. Optical micrographs were collected using an Olympus BX51M optical microscope equipped with an Olympus Qcolor 3 digital microscope camera. Resistance measurements were obtained using a Keithley 2601A Source meter. nTP Au wires were subjected to linear strains on a Micro-Vice stretcher, S.T. Japan, USA, Inc. and resistance was measured at intervals of 5% elongation. The tape test was performed using ASTM standard Permacel tape. The tape was applied to the surface of nTP Au films on T-IIR, pressed for 10 seconds, and then removed. The surface of the nTP Au film on T-IIR and the surface of the tape were subsequently examined using optical microscopy. AFM images were obtained using a Digital Instruments Multimode atomic force microscope in tapping mode. The measurements were carried out using Veeco type FESP cantilever with a nominal tip radius of 8 nm and a nominal force constant of 2.8 N/m. AFM images were collected over a 13 μm x 13 μm

scan area using a scan rate of 0.5 Hz and a scanning resolution of 512 samples/line. RMS roughness values from three different areas of a sample were averaged.

Results and Discussion

Plasma Oxidation of T-IIR T-IIR is a naturally hydrophobic material with a static water contact angle of 95.5 ± 2.3°. We exposed T-IIR surfaces to oxygen plasma for times ranging from 6 to 20 minutes and monitored the hydrophilicity of the surface by measuring contact angles (Figure 1). Oxygen plasma treatment for 6 to 13 minutes initially decreases the water contact angle to ~68°; however, this decrease is due to the expected formation of oxidized bond scission products that remain physisorbed on the surface. We found that swabbing the surface with isopropanol easily removes these products to reveal an unoxidized T-IIR surface with a water contact angle close to the initial value of ~95°. Increasing the oxidation time to ≥ 15 minutes, however, is enough to chemically change the underlying interface. After 15 minutes of plasma oxidation, the water contact angle initially decreases to 47.8 ± 3.2°; after swabbing, the surface remains hydrophilic with a contact angle of 74.6 ± 1.7°. We designate this surface as T-IIR$_{[ox]}$. The contact angle of T-IIR$_{[ox]}$ is consistent with the presence of polar groups at the surface, albeit in low density, which likely comprise a heterogeneous mixture of oxidized functional groups (e.g., -OH, -COOH, ketone) (Scheme 1b). The ATR-FTIR spectrum of T-IIR$_{[ox]}$ appears relatively unchanged from that of native T-IIR, which is expected given the low surface density of oxidized groups indicated by the contact angle (Figure 2a, b). The slight increase in intensity of the broad peak in the region of 3100-3550 cm^{-1}, which corresponds to O-H stretching vibrations, could be due to the introduction of surface hydroxyl groups; however, the broadness of the O-H stretching

region and possible differences in the amount of physisorbed water on the surface makes these intensity comparisons unreliable.

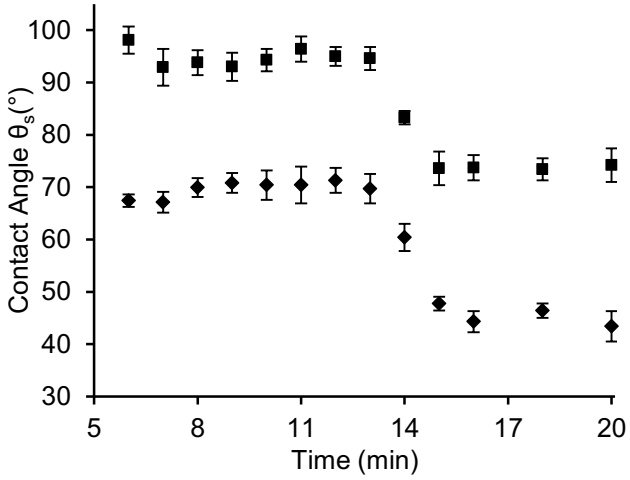

Figure 1. Static water contact angles of T-IIR (diamonds) and T-IIR swabbed with isopropanol (squares) as a function of exposure time to oxygen plasma

Silicate Layer Formation on T-IIR$_{[ox]}$ The low density of polar groups formed from plasma oxidation of T-IIR produces a surface that is neither highly wettable nor suitable for subsequent reactions with organosilanes for surface modification. We therefore implemented an additional surface treatment to increase the density of surface hydroxyl groups on the T-IIR$_{[ox]}$ surface. The T-IIR$_{[ox]}$ surface is similar to the unselectively oxidized surface produced from plasma oxidation of polyethylene (PE).[31] Ferguson *et al.* demonstrated that exposure of this surface to $SiCl_4$ vapor in humid air results in the formation of a continuous layer of hydrated SiO_2 on the surface with a thickness of approximately 200 - 1000 Å depending on the humidity conditions.[31] This silicate layer is chemically similar to the surface of oxidized PDMS, and can support the formation of organosilane SAMs. We applied this treatment to T-IIR$_{[ox]}$ to generate T-IIR$_{[ox]}$/SiO_2 (Scheme 1b), and found that the formation of the SiO_2 layer provides a hydrophilic, -OH terminated surface

that does not compromise the transparency of the material. The water contact angle on T-IIR$_{[ox]}$/SiO$_2$ is < 20°, and the broad peak at 3100-3550 cm^{-1} in the ATR-FTIR spectrum can be attributed to O-H stretching vibrations of the hydroxyl-terminated SiO$_2$ layer (Figure 2c). The X-ray photoelectron spectroscopy (XPS) survey scan of T-IIR$_{[ox]}$/SiO$_2$ shows peaks due to oxygen, carbon, and phosphorus, consistent with the formulation of T-IIR, along with the 2s and 2p peaks of silicon attributed to the SiO$_2$ layer (Figure 3a). AFM imaging of the T-IIR$_{[ox]}$/SiO$_2$ surface reveals that plasma oxidation and SiCl$_4$ treatment roughens the surface from a root-mean-square (RMS) roughness of 3.9 ± 0.6 nm for native T-IIR to 40.5 ± 8.7 nm for T-IIR$_{[ox]}$/SiO$_2$ (Figure S1). This tenfold increase in roughness is similar to the roughness increase due to plasma oxidation of PDMS (from 2.7 nm for native PDMS to 25.5 nm for oxidized PDMS).[47] Nonetheless, the transmittance of T-IIR$_{[ox]}$/SiO$_2$ (72.1% at 550 nm) remains relatively unchanged compared to native T-IIR (74.9% at 550 nm) (Figure S2).

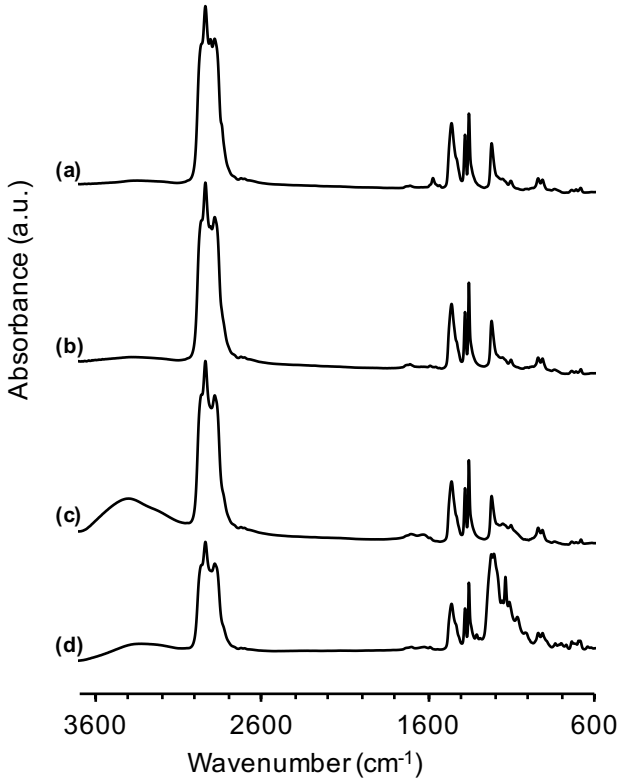

Figure 2. ATR-FTIR spectra of (a) native T-IIR, (b) T-$IIR_{[ox]}$, (c) T-$IIR_{[ox]}/SiO_2$, and (d) T-$IIR_{[ox]}/SiO_2$/FOTS

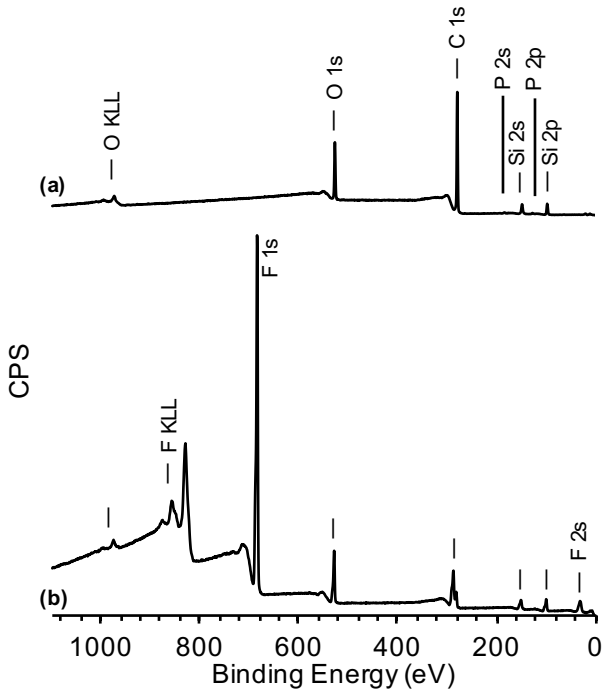

Figure 3. XPS survey scans of (a) T-$IIR_{[ox]}/SiO_2$, and (b) T-$IIR_{[ox]}/SiO_2$/FOTS

SAM Formation on T-$IIR_{[ox]}/SiO_2$ Similar to oxidized PDMS, T-$IIR_{[ox]}/SiO_2$ readily reacts with trichloro- and trialkoxyorganosilanes to chemisorb an organosilane layer on the surface. We deposited organosilane SAMs with a variety of terminal groups on the surface of T-$IIR_{[ox]}/SiO_2$ as a proof of concept to demonstrate the successful surface modification of T-IIR. Exposing T-$IIR_{[ox]}/SiO_2$ to 3-aminopropyltriethoxysilane (APTES), *n*-octadecyltrichlorosilane (OTS), 3-mercaptopropyltrimethoxysilane (MPTMS), and (1H,1H,2H,2H-perfluorooctyl)trichlorosilane (FOTS) yields SAMs with contact angles that are typical of each of these layers (Table 1).[48-51] We further characterized the FOTS SAM on T-$IIR_{[ox]}/SiO_2$ (T-$IIR_{[ox]}/SiO_2$/FOTS) using XPS and ATR-FTIR spectroscopy. The XPS survey scan of T-$IIR_{[ox]}/SiO_2$/FOTS shows peaks due to

silicon, oxygen, and carbon, as well as the 1s and 2s peaks of fluorine (Figure 3b). The FTIR-ATR spectrum of T-IIR$_{[ox]}$/SiO$_2$/FOTS (Figure 2d, 4a) shows C-F stretching bands in the region of 1000-1400 cm^{-1}, confirming the presence of FOTS molecules on the surface. Furthermore, the signal due to O-H stretching at 3100-3550 cm^{-1} in the FTIR-ATR spectrum of T-IIR$_{[ox]}$/SiO$_2$ diminishes upon formation of the FOTS SAM, consistent with the reaction of the surface hydroxyl groups with FOTS to form Si-O-Si bonds to the surface.

Table 1. Static water contact angles of SAMs formed on T-IIR$_{[ox]}$/SiO$_2$.

SAM	θ (H_2O) (°)
T-IIR$_{[ox]}$/SiO$_2$/APTES	53.4 ± 6.0
T-IIR$_{[ox]}$/SiO$_2$/OTS	101.2 ± 0.9
T-IIR$_{[ox]}$/SiO$_2$/FOTS	107.5 ± 2.0
T-IIR$_{[ox]}$/SiO$_2$/MPTMS	64.7 ± 1.1

We treated T-IIR$_{[ox]}$ substrates with FOTS to confirm that the SiO$_2$ layer of T-IIR$_{[ox]}$/SiO$_2$ is necessary for SAM formation. The water contact angle of T-IIR$_{[ox]}$/FOTS of 99.8 ± 1.1° and the C-F stretching vibration at 1148 cm^{-1} in the ATR-FTIR spectrum (Figure 4c) indicate that FOTS is present on the surface; however, both the water contact angle and the intensity of the C-F peak are lower compared to those of T-IIR$_{[ox]}$/SiO$_2$/FOTS. Furthermore, rinsing T-IIR$_{[ox]}$/FOTS with toluene results in the loss of C-F stretching peaks in the ATR-FTIR spectrum (Figure 4d), whereas the T-IIR$_{[ox]}$/SiO$_2$/FOTS spectrum remains unchanged (Figure 4b). Based on these results, we conclude that the SiO$_2$ layer is essential to covalently anchor the FOTS layer, enabling

chemisorption of FOTS adsorbates. Omitting the SiO_2 layer results in the formation of a physisorbed FOTS layer that can easily be removed by rinsing.

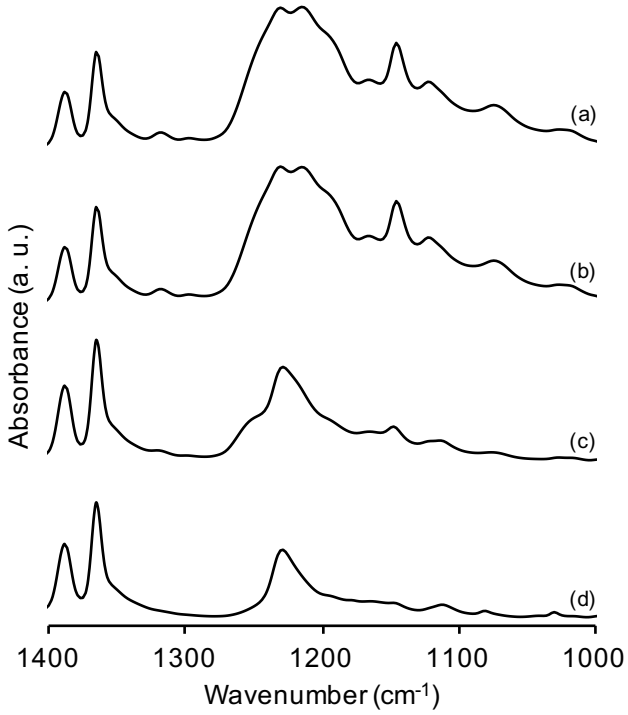

Figure 4. ATR-FTIR spectra of the 1400-1000 cm^{-1} region of (a) T-$IIR_{[ox]}$/SiO_2/FOTS, (b) T-$IIR_{[ox]}$/SiO_2/FOTS after rinsing with toluene, (c) T-$IIR_{[ox]}$/FOTS, and (d) T-$IIR_{[ox]}$/FOTS after rinsing with toluene.

Fabrication of Stretchable Gold Films on T-$IIR_{[ox]}$/SiO_2 The chemisorption of functionalized silanes on T-$IIR_{[ox]}$/SiO_2 provides robust functional surfaces for the deposition of electronic materials and subsequent fabrication of stretchable electronics. As a proof of concept, we demonstrate the fabrication of a stretchable wire using an MPTMS SAM on T-$IIR_{[ox]}$/SiO_2 to bind a gold film to the surface. MPTMS is a well-known molecular adhesive used to bind gold films to oxide surfaces through the formation of covalent gold-sulfur bonds at one end of the

molecule and Si-O bonds to the oxide surface at the other.[33,52] MPTMS is a key component of nanotransfer printing (nTP), an additive printing process in which a PDMS stamp is first coated with a film of gold by e-beam evaporation, and then brought into conformal contact with a target substrate functionalized with MPTMS.[34,52] Covalent Au-S bonds form at the gold-MPTMS interface, causing the gold film to remain adhered to the surface when the PDMS stamp is subsequently peeled away.[33-34,52] We used nTP to transfer gold films from a PDMS stamp to T-$IIR_{[ox]}/SiO_2$/MPTMS (Scheme 2). The transferred gold films exhibit good adhesion to the T-$IIR_{[ox]}/SiO_2$/MPTMS surface and pass the tape test without transfer of gold to the surface of the tape. Optical micrographs and resistivity measurements indicate that nTP transfers gold films that are intact and undamaged to the T-$IIR_{[ox]}/SiO_2$/MPTMS surface: Optical micrographs of gold films transferred to T-$IIR_{[ox]}/SiO_2$/MPTMS from a flat PDMS stamp reveal uniform gold films without cracks or discontinuities (Figure 5a); furthermore, the resistivity of the transferred gold films ($2.9 \pm 0.8 \times 10^{-8}$ Ω m) is equivalent to that of bulk gold (2.3×10^{-8} Ω m).[53] We also transferred patterned gold films to T-$IIR_{[ox]}/SiO_2$/MPTMS using microstructured PDMS stamps. In this process, only the raised regions of gold-coated microstructured PDMS stamps come into contact with the T-$IIR_{[ox]}/SiO_2$/MPTMS surface, creating a patterned film after removal. We transferred gold films with arrays of 20 μm x 20 μm square-shaped holes spaced 20 μm apart (Figure 5b) and 100 μm apart (Figure 5c); 50 μm x 50 μm square-shaped holes spaced 250 μm apart (Figure 5d); 20-μm-wide gold lines with 20-μm-wide spaces (Figure 5e); and 50-μm-wide gold lines with 50-μm-wide spaces (Figure 5f).

Scheme 2. Nano-transfer printing of a gold film from a PDMS stamp to the surface of T-IIR$_{[ox]}$/SiO$_2$/MPTMS.

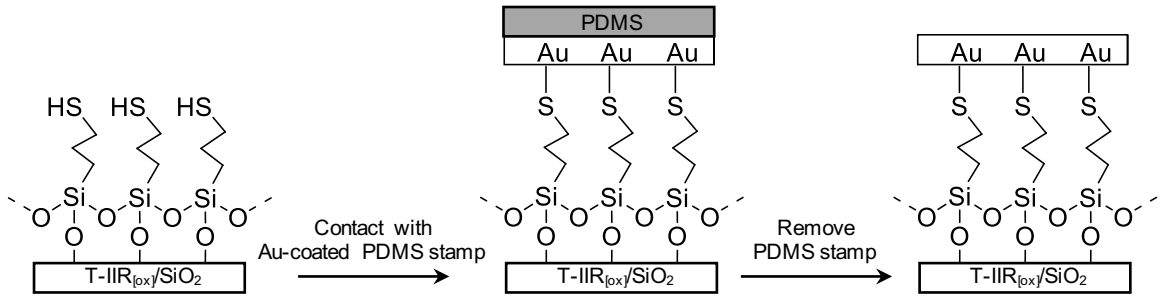

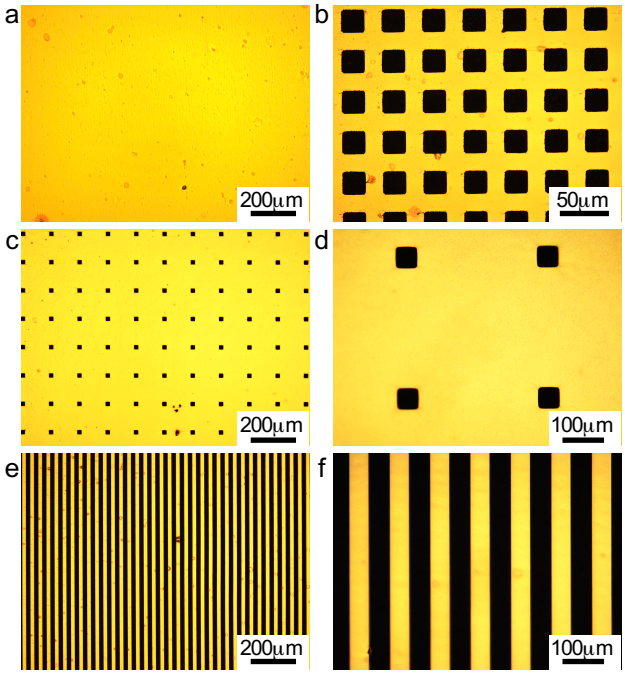

Figure 5. Optical micrographs of gold films prepared by nTP on T-IIR$_{[ox]}$/SiO$_2$/MPTMS using (a) a flat PDMS stamp; and patterned PDMS stamps to produce gold films with (b) 20 μm x 20 μm square-shaped holes spaced 20 μm apart; (c) 20 μm x 20 μm square-shaped holes spaced 100 μm apart; (d) 50 μm x 50 μm square-shaped holes spaced 250 μm apart; (e) 20-μm-wide gold lines with 20-μm-wide spaces; and (f) 50-μm-wide gold lines with 50-μm-wide spaces.

Stretchable metal films are important elements of stretchable electronics, where they are used as device electrodes and interconnects. A typical fabrication method uses e-beam evaporation to deposit a thin layer of titanium or chromium metal as an adhesion layer onto a PDMS substrate, followed by gold. These PDMS/gold wires develop cracks with stretching, which interrupt the conductivity at 23% elongation.[15] We characterized nTP Au wires (1 mm x 10 mm) on T-$IIR_{[ox]}/SiO_2$/MPTMS by measuring the electrical resistance as a function of elongation. A plot of the percentage change in resistance as a function of elongation (Figure 6) shows that the nTP gold wires remain conductive to 20% elongation. Beyond this point, the resistance becomes essentially infinite; however, the nTP gold wires regain conductivity with $(R-R_0)/R_0 = 14.5 \pm 2.5\%$ after releasing the strain. This performance is similar to that of the reported gold wires deposited on PDMS using e-beam evaporation:[15] Both structures exhibit a change in resistance of ~900% at 20% elongation and become non-conductive at higher strains.

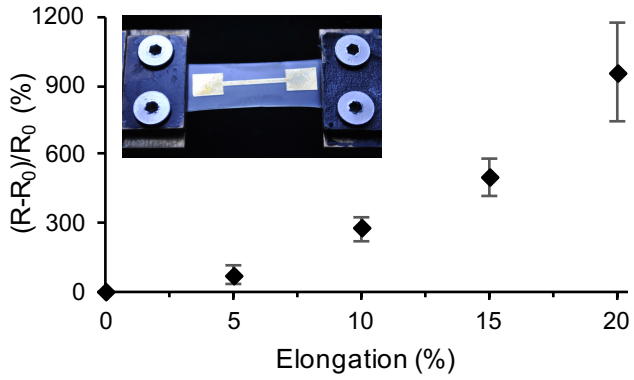

Figure 6. Percentage change in resistance of nTP Au wires as a function of elongation, with a photograph of a stretched nTP Au wire on T-$IIR_{[ox]}/SiO_2$/MPTMS stretched to 20% (inset).

Conclusions

T-IIR has the potential to revolutionize the field of stretchable electronics. Its excellent gas-barrier properties protect sensitive organic electronic devices from degradation due to oxygen and moisture, which provides a route to stretchable devices with practical lifetimes. The surface modification methods developed here are critically important to advancing T-IIR from a conformable device encapsulant to a substrate for the direct fabrication of stretchable devices. The combination of plasma treatment and chemical surface modification described here can customize the wettability and chemical properties of the T-IIR surface to enable the deposition of a variety of functional materials, opening the way to robust, stretchable devices.

Corresponding Author

*E-mail: tbcarmic@uwindsor.ca.

Acknowledgements

This research was supported by the National Sciences and Engineering Research Council of Canada (NSERC) and LANXESS, Inc. We thank Dr. Mark Biesinger at Surface Science Western for X-ray photoelectron spectroscopy.

Table of Contents Graphic (3.25 inches by 1.75 inches)

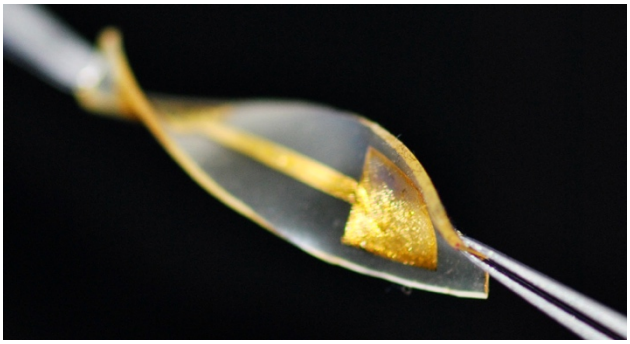

References

(1) Rogers, J. A.; Someya, T.; Huang, Y., Materials and Mechanics for Stretchable Electronics. *Science* **2010,** *327*, 1603–1607.

(2) Bauer, S.; Bauer-Gogonea, S.; Graz, I.; Kaltenbrunner, M.; Keplinger, C.; Schwodiauer, R., 25th Anniversary Article: A Soft Future: From Robots and Sensor Skin to Energy Harvesters. *Adv. Mater.* **2014,** *26*, 149–161.

(3) Filiatrault, H. L.; Porteous, G. C.; Carmichael, R. S.; Davidson, G. J.; Carmichael, T. B., Stretchable Light-Emitting Electrochemical Cells Using an Elastomeric Emissive Material. *Adv. Mater.* **2012,** *24*, 2673–2678.

(4) Liang, J.; Li, L.; Niu, X.; Yu, Z.; Pei, Q., Elastomeric Polymer Light-Emitting Devices and Displays. *Nature Photon.* **2013,** *7*, 817–824.

(5) Wang, J.; Yan, C.; Chee, K.; Lee, P., Highly Stretchable and Self-Deformable Alternating Current Electroluminescent Devices. *Adv. Mater.* **2015,** *27*, 2876–2882.

(6) Vosgueritchian, M.; Tok, J. B. H.; Bao, Z., Stretchable LEDs: Light-Emitting Electronic Skin. *Nature Photon.* **2013,** *7*, 769–771.

(7) Sekitani, T.; Nakajima, H.; Maeda, H.; Fukushima, T.; Aida, T.; Hata, K.; Someya, T., Stretchable Active-Matrix Organic Light-Emitting Diode Display Using Printable Elastic Conductors. *Nature Mater.* **2009,** *8*, 494–499.

(8) Lipomi, D. J.; Tee, B. C.; Vosgueritchian, M.; Bao, Z., Stretchable Organic Solar Cells. *Adv. Mater.* **2011,** *23*, 1771–1775.

(9) Kim, D. H.; Lu, N.; Ma, R.; Kim, Y. S.; Kim, R. H.; Wang, S.; Wu, J.; Won, S. M.; Tao, H.; Islam, A.; Yu, K. J.; Kim, T. I.; Chowdhury, R.; Ying, M.; Xu, L.; Li, M.; Chung, H. J.; Keum, H.; McCormick, M.; Liu, P.; Zhang, Y. W.; Omenetto, F. G.; Huang, Y.; Coleman, T.; Rogers, J. A., Epidermal Electronics. *Science* **2011,** *333*, 838–843.

(10) Hammock, M. L.; Chortos, A.; Tee, B. C.; Tok, J. B.; Bao, Z., 25th Anniversary Article: The Evolution of Electronic Skin (E-Skin): A Brief History, Design Considerations, and Recent Progress. *Adv. Mater.* **2013,** *25*, 5997–6038.

(11) Huang, X.; Liu, Y.; Cheng, H.; Shin, W.-J.; Fan, J. A.; Liu, Z.; Lu, C.-J.; Kong, G.-W.; Chen, K.; Patnaik, D.; Lee, S.-H.; Hage-Ali, S.; Huang, Y.; Rogers, J. A., Materials and Designs for Wireless Epidermal Sensors of Hydration and Strain. *Adv. Funct. Mater.* **2014,** *24*, 3846–3854.

(12) Kim, D. H.; Ghaffari, R.; Lu, N.; Rogers, J. A., Flexible and Stretchable Electronics for Biointegrated Devices. *Annu. Rev. Biomed. Eng.* **2012,** *14*, 113–128.

(13) Cheng, T.; Zhang, Y.; Lai, W. Y.; Huang, W., Stretchable Thin-Film Electrodes for Flexible Electronics with High Deformability and Stretchability. *Adv. Mater.* **2015,** *27*, 3349–3376.

(14) Graudejus, O.; Gorrn, P.; Wagner, S., Controlling the Morphology of Gold Films on Poly(dimethylsiloxane). *ACS Appl. Mater. Interfaces* **2010,** *2*, 1927–1933.

(15) Lacour, S. P.; Wagner, S.; Huang, Z.; Suo, Z., Stretchable Gold Conductors on Elastomeric Substrates. *Appl. Phys. Lett.* **2003,** *82*, 2404–2406.

(16) Filiatrault, H. L.; Carmichael, S. R.; Boutette, R. A.; Carmichael, T., A Self-Assembled, Low-Cost, Microstructured Layer for Extremely Stretchable Gold Films. *ACS Appl. Mater. Interfaces* **2015,** *7*, 20745–20752.

(17) Guo, R.; Yu, Y.; Zeng, J.; Liu, X.; Zhou, X.; Niu, L.; Gao, T.; Li, K.; Yang, Y.; Zhou, F.; Zheng, Z., Biomimicking Topographic Elastomeric Petals (E-Petals) for Omnidirectional Stretchable and Printable Electronics. *Adv. Sci.* **2015,** *2*, 1400021.
(18) Kim, D.-H.; Rogers, J. A., Stretchable Electronics: Materials Strategies and Devices. *Adv. Mater.* **2008,** *20*, 4887–4892.
(19) Khang, D.-Y.; Rogers, J. A.; Lee, H. H., Mechanical Buckling: Mechanics, Metrology, and Stretchable Electronics. *Adv. Funct. Mater.* **2009,** *19*, 1526–1536.
(20) Zhang, Y.; Yan, Z.; Nan, K.; Xiao, D.; Liu, Y.; Luan, H.; Fu, H.; Wang, X.; Yang, Q.; Wang, J.; Ren, W.; Si, H.; Liu, F.; Yang, L.; Li, H.; Wang, J.; Guo, X.; Luo, H.; Wang, L.; Huang, Y.; Rogers, J. A., A Mechanically Driven Form of Kirigami as a Route to 3D Mesostructures in Micro/Nanomembranes. *Proc. Natl. Acad. Sci. U.S.A.* **2015,** *112*, 11757–11764.
(21) Zhu, Y.; Moran-Mirabal, J., Highly Bendable and Stretchable Electrodes Based on Micro/Nanostructured Gold Films for Flexible Sensors and Electronics. *Adv. Elec. Mater.* **2016,** *2*, 1500345.
(22) Fan, J. A.; Yeo, W. H.; Su, Y.; Hattori, Y.; Lee, W.; Jung, S. Y.; Zhang, Y.; Liu, Z.; Cheng, H.; Falgout, L.; Bajema, M.; Coleman, T.; Gregoire, D.; Larsen, R. J.; Huang, Y.; Rogers, J. A., Fractal Design Concepts for Stretchable Electronics. *Nature Commun.* **2014,** *5*, 3266.
(23) Savagatrup, S.; Printz, A. D.; O'Connor, T. F.; Zaretski, A. V.; Lipomi, D. J., Molecularly Stretchable Electronics. *Chem. Mater.* **2014,** *26*, 3028–3041.
(24) Lipomi, D. J., Stretchable Figures of Merit in Deformable Electronics. *Adv. Mater.* **2016,** *28*, 4180–4183.
(25) Suo, Z., Mechanics of Stretchable Electronics and Soft Machines. *MRS Bull.* **2012,** *37*, 218–225.
(26) Lu, N.; Wang, X.; Suo, Z.; Vlassak, J., Metal Films on Polymer Substrates Stretched Beyond 50%. *Appl. Phys. Lett.* **2007,** *91*, 221909.
(27) Morent, R.; De Geyter, N.; Axisa, F.; De Smet, N.; Gengembre, L.; De Leersnyder, E.; Leys, C.; Vanfleteren, J.; Rymarczyk-Machal, M.; Schacht, E.; Payen, E., Adhesion Enhancement by a Dielectric Barrier Discharge of PDMS Used for Flexible and Stretchable Electronics. *J. Phys. D: Appl. Phys.* **2007,** *40*, 7392–7401.
(28) Xiang, Y.; Li, T.; Suo, Z.; Vlassak, J. J., High Ductility of a Metal Film Adherent on a Polymer Substrate. *Appl. Phys. Lett.* **2005,** *87*, 161910.
(29) Mark, J. E.; Schaefer, D. W.; Lin, G., *The Polysiloxanes*. Oxford University Press: New York, **2015**.
(30) Chaudhary, M. K.; Whitesides, G. M., Direct Measurement of Interfacial Interactions between Semispherical Lenses and Flat Sheets of Poly(dimethylsiloxane) and Their Chemical Derivatives. *Langmuir* **1991,** *7*, 1013–1025.
(31) Ferguson, G. S.; Chaudhury, M. K.; Biebuyck, H. A.; Whitesides, G. M., Monolayers on Disordered Substrates: Self-Assembly of Alkyltrichlorosilanes on Surface-Modified Polyethylene and Poly(dimethylsiloxane). *Macromol.* **1993,** *26*, 5870–5875.
(32) Chaudhary, M. K.; Whitesides, G. M., Correlation between Surface Free Energy and Surface Constitution. *Science* **1992,** *255*, 1230–1232.
(33) Byun, I.; Coleman, A. W.; Kim, B., Transfer of Thin Au Films to Poly(dimethylsiloxane) (PDMS) with Reliable Bonding Using (3-Mercaptopropyl)trimethoxysilane (MPTMS) as a Molecular Adhesive. *J. Micromech. Microeng.* **2013,** *23*, 085016.

(34) Carlson, A.; Bowen, A. M.; Huang, Y.; Nuzzo, R. G.; Rogers, J. A., Transfer Printing Techniques for Materials Assembly and Micro/Nanodevice Fabrication. *Adv. Mater.* **2012,** *24*, 5284–5318.
(35) Miller, M. S.; Davidson, G. J. E.; Sahli, B. J.; Mailloux, C. M.; Carmichael, T. B., Fabrication of Elastomeric Wires by Selective Electroless Metallization of Poly(dimethylsiloxane). *Adv. Mater.* **2008,** *20*, 59–64.
(36) Vohra, A.; Imin, P.; Imit, M.; Carmichael, R. S.; Meena, J. S.; Adronov, A.; Carmichael, T. B., Transparent, Stretchable, and Conductive SWNT Films Using Supramolecular Functionalization and Layer-by-Layer Self-Assembly. *RSC Advances* **2016,** *6*, 29254–29263.
(37) Jones, D. M.; Huck, W. T. S., Controlled Surface-Initiated Polymerizations in Aqueous Media. *Adv. Mater.* **2001,** *13*, 1256–1259.
(38) Yu, Y.; Yan, C.; Zheng, Z., Polymer-Assisted Metal Deposition (PAMD): A Full-Solution Strategy for Flexible, Stretchable, Compressible, and Wearable Metal Conductors. *Adv. Mater.* **2014,** *26*, 5508–5516.
(39) Vohra, A.; Filiatrault, H. L.; Amyotte, S. D.; Carmichael, R. S.; Suhan, N. D.; Siegers, C.; Ferrari, L.; Davidson, G. J. E.; Carmichael, T. B., Reinventing Butyl Rubber for Stretchable Electronics. *Adv. Funct. Mater.* **2016,** *26*, 5222–5229.
(40) Scholz, S.; Kondakov, D.; Lussem, B.; Leo, K., Degradation Mechanisms and Reactions in Organic Light-Emitting Devices. *Chem. Rev.* **2015,** *115*, 8449–8503.
(41) Soltzberg, L., J.; Slinker, J., D.; Flores-Torres, S.; Bernards, D. A.; Malliaras, G. G.; Abruña, H. D.; Kim, J.-S.; Friend, R. H.; Kaplan, M. D.; Goldberg, V., Identification of a Quenching Species in Ruthenium Tris-Bipyridine Electroluminescent Devices. *J. Am. Soc. Chem* **2006,** *128*, 7761–7764.
(42) Hauch, J. A.; Schilinsky, P.; Choulis, S. A.; Rajoelson, S.; Brabec, C. J., The Impact of Water Vapor Transmission Rate on the Lifetime of Flexible Polymer Solar Cells. *Appl. Phys. Lett.* **2008,** *93*, 103306.
(43) Iyengar, Y., Relation of Water Vapor Permeability of Elastomers to Molecular Structure. *J. Polym. Sci. B: Polym. Lett.* **1965,** *3*, 663–669.
(44) George, S. C.; Thomas, S., Transport Phenomena through Polymeric Systems. *Prog. Polym. Sci.* **2001,** *26*, 985–1017.
(45) Crowther, B. G. E., *Handbook of Rubber Bonding*. Rapra Technology Limited: Shawbury, Shrewbury, Shropshire, **2001**.
(46) Qin, D.; Xia, Y.; Whitesides, G. M., Soft Lithography for Micro- and Nanoscale Patterning. *Nature Protoc.* **2010,** *5*, 491–502.
(47) Maheshwari, N.; Kottantharayil, A.; Kumar, M.; Mukherji, S., Long Term Hydrophilic Coating on Poly(dimethylsiloxane) Substrates for Microfluidic Applications. *Appl. Surf. Sci.* **2010,** *257*, 451–457.
(48) Zeng, X.; Xu, G.; Gao, Y.; An, Y., Surface Wettability of (3-Aminopropyl)triethoxysilane Self-Assembled Monolayers. *J. Phys. Chem. B* **2011,** *115*, 450–454.
(49) Dong, J.; Wang, A.; Ng, K. Y. S.; Mao, G., Self-Assembly of Octadecyltrichlorosilane Monolayers on Silicon-Based Substrates by Chemical Vapor Deposition. *Thin Solid Films* **2006,** *515*, 2116–2122.

(50) Pavlovic, E.; Quist, A. P.; Gelius, U.; Oscarsson, S., Surface Functionalization of Silicon Oxide at Room Temperature and Atmospheric Pressure. *J. Coll. Inter. Sci.* **2002,** *254*, 200–203.
(51) Hozumi, A.; Ushiyama, K.; Sugimura, H.; Takai, O., Fluoroalkylsilane Monolayers Formed by Chemical Vapor Surface Modification on Hydroxylated Oxide Surfaces. *Langmuir* **1999,** *15*, 7600–7604.
(52) Loo, Y.-L.; Willett, R. L.; Baldwin, K. W.; Rogers, J. A., Interfacial Chemistries for Nanoscale Transfer Printing. *J. Am. Chem. Soc.* **2002,** *124*, 7654–7655.
(53) McCoul, D.; Weili, H.; Gao, M.; Vishrut, M.; Pei, Q., Recent Advances in Stretchable and Transparent Electronic Materials. *Adv. Elec. Mater.* **2016,** *2*, 1500407.